1 Materials and characterizations

1.1 Materials

The scrapped explosive tear gas grenades were obtained from Henan Hong Shang Yu Industrial Co., Ltd. Methanol, trichloromethane, ethanol, acetone, acetonitrile and other solvents were purchased from Macklin Biochemical Technology Co., Ltd, Shanghai. And drugs such as o-phenylenediamine, hydrochloric acid, sodium formate, and sodium bisulfite were gained from Sinopharm Group, China. Ultrapure water used in the experiment was produced by an ultrapure water machine (UPT-II-10 T).

1.2 Characterizations

The surface morphology of the samples was characterized using scanning electron microscope (SEM) (Hitachi SU8010, Japan). The chemical composition and functional group analysis were performed with Fourier transform infrared (FTIR) spectrometer (Thermo Fisher Scientific Nicolet iS20, USA). Thermogravimetric analysis was carried out on a thermal analyzer (NETZSCH STA2500, Germany), recording the mass changes during programmed heating to analyze the thermal decomposition behavior. The melting range of the recycled product was determined using a melting point apparatus (WRS-2C, China), providing a preliminary evaluation of product purity.

The chemical structure was confirmed by analyzing the ^{13}C and ^{1}H nuclear magnetic resonance (NMR) spectra (Bruker AV-400, Germany), thereby verifying the recycled product. For ^{1}H NMR spectra, tetramethylsilane (TMS) was used as the internal reference (0.0 ppm). The chemical shifts for the solvents were reported relative to the residual solvent peaks: $CDCl_3$ at 7.26 ppm and DMSO-d_6 at 2.5 ppm. For ^{13}C NMR spectra, the central peak of the solvent multiplet was used as the reference: $CDCl_3$ at 77.0 ppm and DMSO-d_6 at 39.4 ppm.

The recycled and synthesized products were analyzed using a Q Exactive high-performance liquid chromatography-mass spectrometer (HPLC-MS) (Thermo Scientific, Germany). The mass spectrometry conditions were set as follows: an atmospheric pressure chemical ionization (APCI) source, positive ion scanning mode, sheath gas pressure of 45 psi, auxiliary gas flow rate of 15 L/min, ion source temperature of 300 °C, capillary temperature of 300 °C, and capillary voltage of 3200

V. The analysis was to determine the molecular weight and further verify the recycled production.

1.3 Density functional theory (DFT) calculation details

Quantum chemical calculations were performed using the ORCA software (version 6.0.1) to calculate the reaction energy barriers of intermediates and transition states at various stages. Geometry optimizations were conducted at the B3LYP-D4/def2-SVP level of theory. To simulate the 50% ethanol/water solution environment, the dielectric constant (epsilon) and refractive index (refrac) were modified in the CPCM input module, and the SMD solvation model was employed. Frequency analyses were carried out to confirm that all stable compounds exhibited no imaginary frequencies, while each transition state had exactly one imaginary frequency. To obtain more accurate electronic energies, single-point energy calculations were performed at the higher level of theory wB97M-V/ma-def2-TZVPP. The calculation temperature was set to 368 K, and a frequency scaling factor of 0.9850 was applied.

2 Extraction methods

2.1 Soxhlet extraction

10 g of the main charge was weighed into a Soxhlet extractor. A certain amount of methanol was poured into a 500 mL single-neck flask. The Soxhlet extractor was then assembled on the single-neck flask and immerse it in a water bath to heat to 60 °C. After extraction, the solid was dried and weighed. The extract was then subjected to vacuum distillation using a rotary evaporator to evaporate and recover the methanol.

2.2 Ultrasonic extraction

10 g of the main charge was weighed into a 500 mL single necked flask, then add 350 mL of methanol. After extraction under ultrasonic condition, a circulating water multi-purpose vacuum pump (SHZ-D9(III), China) was used to filter, and the resulting filter residue was dried and weighed. Using a rotary evaporator (RE-2000B) to perform negative pressure distillation on the filtrate, evaporate and recover methanol.

2.3 Stir extraction

10 g of the main charge was weighed into a 500 mL single-neck flask, then add 350 mL of methanol. Position the flask on a magnetic stirrer and extract at room

temperature for a period of time. After extraction, a circulating water multi-purpose vacuum pump was used for filtration. The resulting filter residue was dried and weighed. Performing vacuum distillation on the filtrate using a rotary evaporator to recover the methanol.

3 Dissolution of the main charge components in different solvents

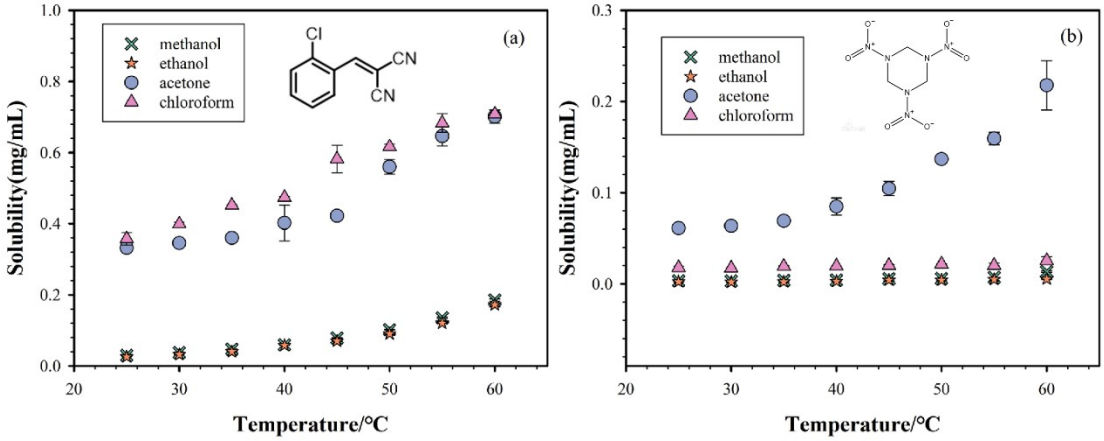

Fig. S1 Scatter plots of the solubility of CS (a) and RDX (b) in different solvents.

Given the high content and intrinsic value of CS and RDX, this study aims to establish efficient methodologies for their separation and recycle from the complex mixture. As shown in Fig. S1, the upper temperature was limited to 60 °C, respecting the boiling points of acetone and chloroform. Results showed a strong positive correlation between temperature and solubility for all solvent-solute pairs. However, the solvents differed significantly in their overall dissolution power and the degree of temperature dependence. For CS, chloroform performed the strongest dissolution capacity. Its solubility increased from 357.5 g/L to 708.3 g/L when the temperature was rose from 25 °C to 60 °C. Methanol and ethanol showed similar tendency, reaching solubilities of 185.7 g/L and 172.3 g/L at 60 °C, corresponding to increases of 53.2% and 48.6% relative to their 25 °C values, respectively. The solubilities of RDX in the different solvents showed significant differences. Acetone exhibited relatively high solubility and greater temperature sensitivity. The solubility increased from 61.2 g/L at 25 °C to 217.9 g/L at 60 °C, with an increase of 256.0%. In contrast, the solubilities in methanol, ethanol, and chloroform were low and the enhancement effect of temperature

was less pronounced.

The results suggested that both chloroform and acetone showed favorable dissolution capacity for CS and RDX. Among them, chloroform could achieve higher efficiency in dissolving CS, while acetone had greater advantage in the solubility of RDX. Therefore, in theory, acetone and chloroform could be prioritized as extraction solvents to enhance recovery efficiency from the main charge.

However, experimental observations revealed that significant blockage occurred during suction filtration after the main charge extracted by acetone and chloroform, leading to a prominent reduction in solid-liquid separation efficiency. Considering the insolubility of PVC in the main charge, it was hypothesized that the filtration blockage was related to the swelling of PVC in these solvents. During the sequential experiments, PVC settled slowly in methanol and ethanol, and the solution gradually clarified. In contrast, significant agglomeration and swelling occurred in acetone and chloroform, resulting in a turbid solution with aggregates suspended in the liquid (Fig.S2). It indicated that PVC could swell in acetone and chloroform, causing the particles to expand and agglomerate. Thereby, it could hinder the solid-liquid separation during filtration. Methanol still exhibited good solubility for both CS (185.7 g/L at 60 °C) and RDX (13.4 g/L at 60 °C) without swelling or agglomeration, ultimately being selected as the extraction solvent.

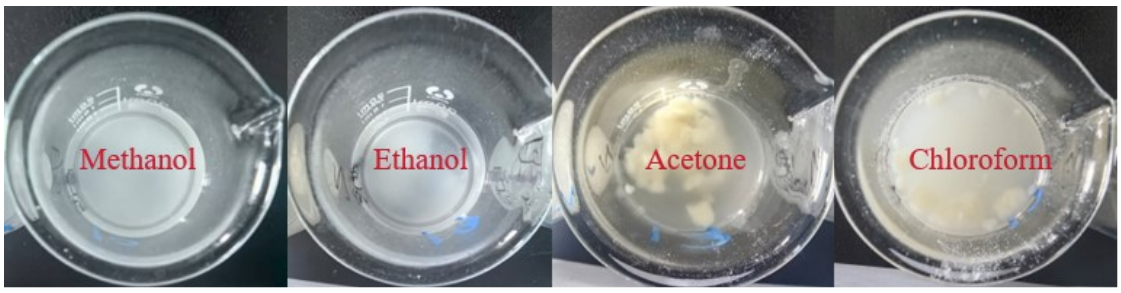

Fig. S2 The state of PVC in different solvents.

Methanol, Chloroform and ethanol are among the most economical organic solvents available industrially. All three solvents have moderate boiling points (methanol: 64.7 °C, chloroform: 61.2 °C, ethanol: 78.4 °C), enabling efficient recovery via rotary evaporation with relatively low energy consumption. As demonstrated in our process, solvent recycling was implemented to minimize waste and reduce operational costs. In addition, the relatively low boiling points of these solvents allow for separation

under mild heating conditions (55 °C for methanol extraction), which is critical when processing thermally sensitive energetic materials like RDX.

Methanol, chloroform, and ethanol are bulk industrial chemicals with stable supply chains, ensuring the scalability and practical applicability of our proposed process.

Several greener solvent alternatives including ethyl acetate (EA), acetonitrile (ACN), acetone (AC) and tetrahydrofuran (THF) have also been conducted preliminary experiments. However, these alternatives showed inferior performance compared to chloroform in the specific system. From Fig. S3, $CHCl_3$ (chloroform, CHL) has a great performance for the separation of RDX, owing to the poorly dissolution for RDX compared with another four solvents.

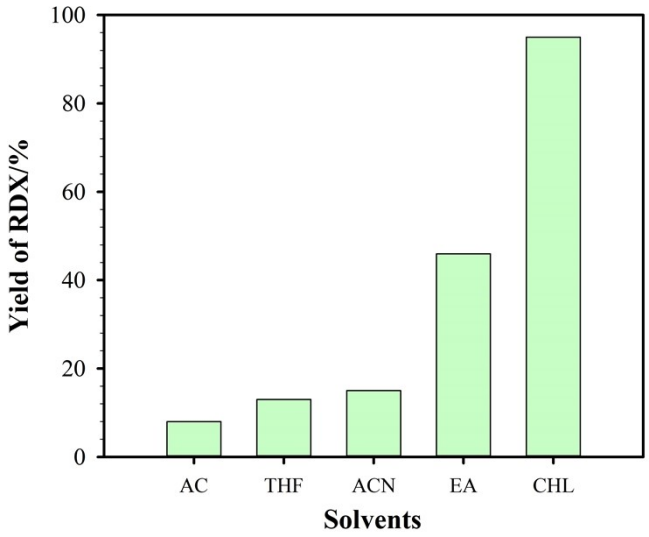

Fig. S3 The influence of different solvents on the yield of RDX.

For RDX, its thermal decomposition onset temperature is above 200 °C (Fig. S4), providing a substantial safety margin for operations at 55–70 °C.

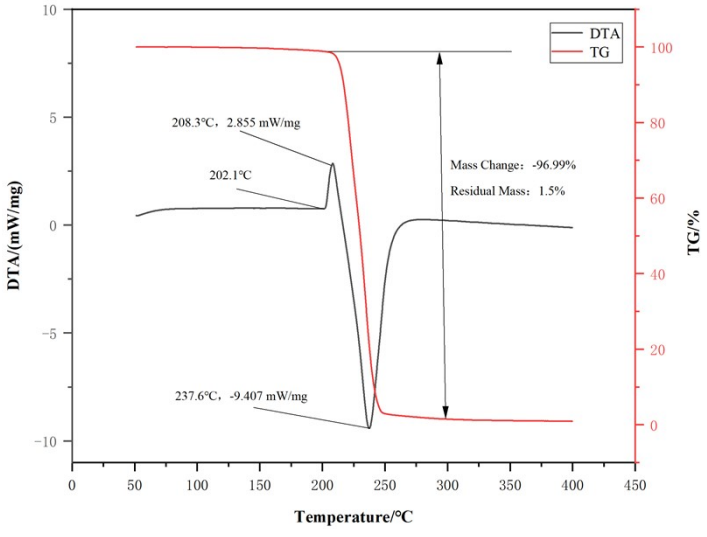

Fig. S4 TG-DTA curves of RDX reference.

As shown in Fig. S5, 500 rpm was determined to be the optimal condition.

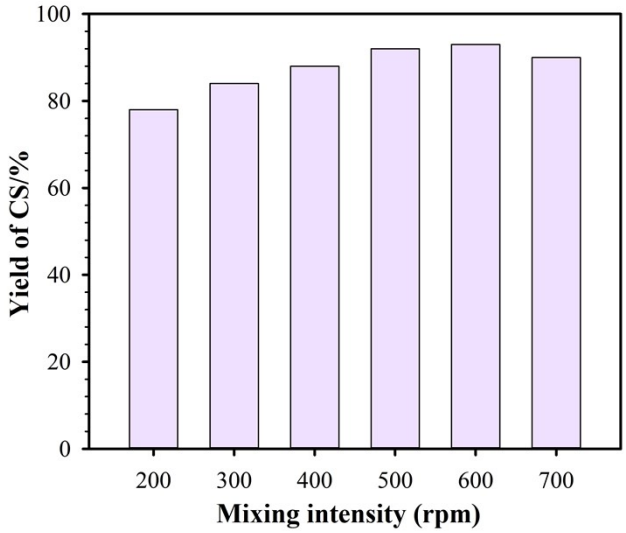

Fig. S5 The influence of mixing intensity on the yield of CS.

As demonstrated in Fig. S6, the solvent maintained its performance over more than three consecutive reuse cycles, highlighting its excellent economic feasibility.

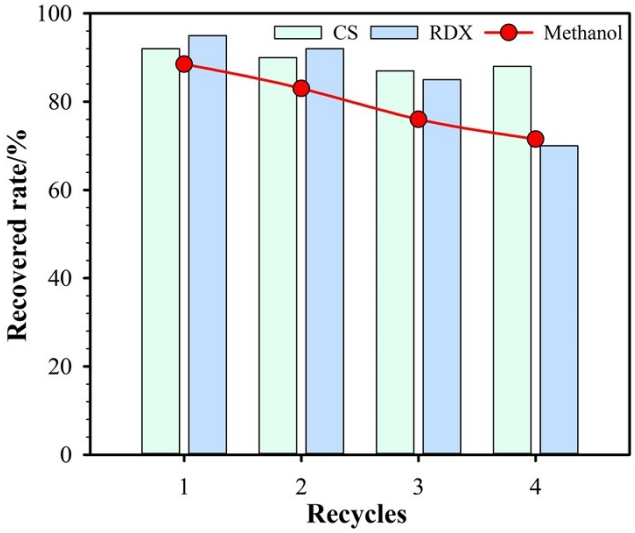

Fig. S6 The influence of solvents recycles on the yield of CS and RDX.

4 The melting point of the recycled sample

Table S1 the melting point of the CS certified reference and the recycled sample.

Samples	Initial melting temperature /°C	Final melting temperature /°C	Melting range	Average Melting range
CS certified	94.7	96.0	1.3	1.33

reference	94.6	96.0	1.4	
	94.9	96.2	1.3	
Recycled sample	94.8	96.1	1.3	
	95.4	96.2	0.8	1.13
	94.9	96.2	1.3	

5 High value conversion process

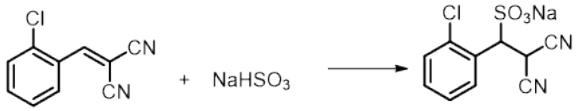

Eq. S1

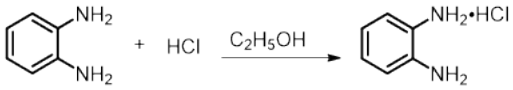

Eq. S2

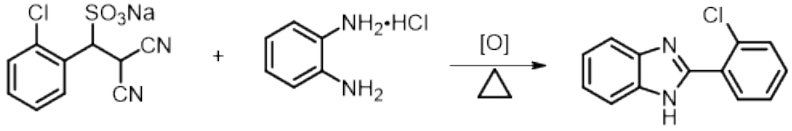

Eq. S3

5.1 Effect of different factors for the transformation of CS

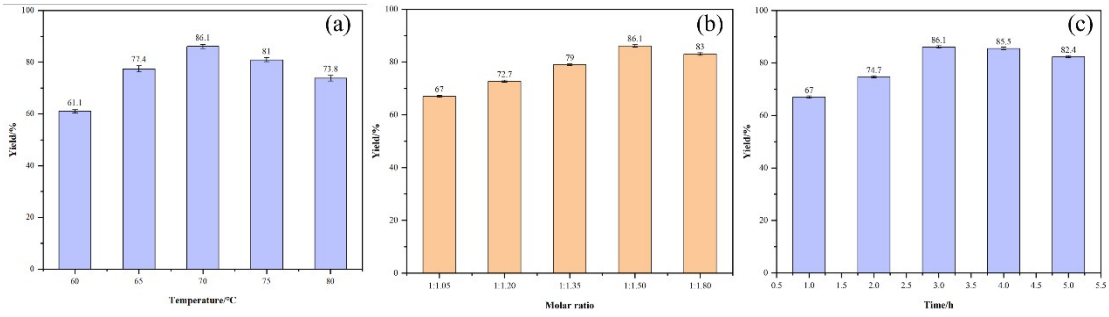

Fig. S7 Effect of different factors to the yield of 2-CPBZ.

The minimal difference (< 2 °C) between onset (233.5 ± 0.5 °C) and completion (234.5 ± 0.5 °C) melting temperatures across all samples indicates highly uniform crystal packing and molecular arrangement. The thermal consistency demonstrates that the synthetic route produces 2-CPBZ with thermodynamic properties equivalent to the certified reference. The narrow melting range further confirms high sample purity and well-defined crystalline structure, validating the robustness of the synthesis process in delivering material with predictable and reproducible thermal characteristics.

Table S2 the melting point of the 2-CPBZ certified reference and the synthetic products.

Samples	Initial melting temperature /℃	Final melting temperature /℃	Melting range	Average Melting range
2-CPBZ certified reference	233.0	233.9	0.9	1.06
	232.4	233.6	1.2	
	232.2	233.3	1.1	
Synthetic products	233.7	234.7	1.0	0.93
	233.0	234.0	1.0	
	233.4	234.2	0.8	

5.2 NMR and GC-MS analysis of 2-CPBZ

In the ^{1}H NMR spectrum of the purified 2-CPBZ, no residual chloroform peak was observed at approximately δ 7.26 ppm, the characteristic chemical shift of $CHCl_3$. It should be noted that the synthesis of 2-CPBZ did not involve chloroform at any step. However, the reviewer correctly notes that chloroform was used during the CS separation stage. Any potential chloroform carryover from this stage is effectively eliminated through the CS purification process, which includes ethanol recrystallization, washing with ice-cold ethanol, and air drying. Chloroform (bp 61.2 °C) is highly volatile and evaporates completely under these conditions. Moreover, even if trace amounts of chloroform remained in the CS starting material, the subsequent synthesis of 2-CPBZ (conducted in an open flask at 70 °C for 3 h) would readily remove any volatile residues.

The 2-CPBZ was analyzed by GC-MS to detect any potential dehalogenation products. The mass spectrum (Fig. 4d) shows a clear molecular ion peak at m/z 227.0 (M+), corresponding to the molecular weight of 2-CPBZ (C13H9ClN2, calculated M=228.68). Importantly, the isotopic pattern exhibits the characteristic 3:1 ratio for the [M]+ and [M+2]+ peaks (m/z 227 and 229), which is definitive evidence for the presence of a single chlorine atom. No significant peak corresponding to the dechlorinated product (m/z 192–193, C13H10N2, calculated M = 194.23) was observed. From a synthetic perspective, the ortho-chlorine substituent is stable under our conditions for two reasons: (1) the C–Cl bond dissociation energy on the benzene ring is far higher than the thermal energy at 70 °C; (2) the chlorine is attached to an aromatic ring, forming p–π conjugation that imparts partial double-bond character, making it more stable than aliphatic C–Cl bonds.

5.3 DFT calculations

Based on the DFT calculations (Fig. 5), the nucleophilic substitution step (compound 2 → TS1) has the highest energy barrier (34.7 kcal/mol) and is therefore identified as the rate-determining step of the overall transformation.

In this system, the oxidative aromatization step occurs spontaneously under aerobic conditions at 70 °C and is thermodynamically driven, with an activation energy lower than that of the rate-determining step. This is consistent with the experimental observation that 2-CPBZ forms readily under the optimized conditions without the need for additional catalysts.

The “activation-energy regulation” did not involve any specific catalyst. Instead, it was achieved through substrate pre-reaction, functional group protection and optimized reaction parameters. CS was converted to its sulfonate adduct, which serves as a better leaving group and lowers the energy barrier for the rate-determining nucleophilic substitution step. OPD was protonated to its monohydrochloride salt, which suppresses oxidative polymerization at 70 °C and ensures controlled reactivity. The 1.5:1 molar ratio ensures sufficient OPD availability for cyclization without promoting side reactions, while the 70 °C temperature provides adequate thermal energy to overcome the activation barriers.